Voltage induced acoustic resonance in metal organic chemical vapor deposition $SrTiO_3$ thin film

Nick M. Sbrockey[a] and Gary S. Tompa
Structured Materials Industries, Inc., Piscataway, New Jersey 08854

Thottam S. Kalkur
Department of Electrical and Computer Engineering, University of Colorado at Colorado Springs, Colorado Springs, Colorado 80933

Jialan Zhang and S. Pamir Alpay
Materials Science and Engineering Program and Institute of Materials Science, University of Connecticut, Storrs, Connecticut 06269

Melanie W. Cole
U.S. Army Research Laboratory, Weapons and Materials Research Directorate, Aberdeen Proving Ground, Maryland 21005

(Received 10 July 2012; accepted 17 September 2012; published 4 October 2012)

A solidly mounted acoustic wave resonator was fabricated using a 150 nm thick $SrTiO_3$ film deposited by metal organic chemical vapor deposition and platinum electrodes deposited by sputtering. The substrate was (0001) sapphire with a multilayer SiO_2/Ta_2O_5 acoustic Bragg reflector. Dielectric characterization of the $SrTiO_3$ film showed low leakage current and the characteristic capacitance–voltage behavior of a paraelectric film. Measurement of the radio frequency transmission characteristics showed no resonance with zero bias voltage across the $SrTiO_3$ film. At 1.0 V applied DC bias, a well defined resonance peak was observed near 5.6 GHz. With increasing voltage across the $SrTiO_3$ film, the resonance increased in intensity and shifted to lower frequency. The calculated electromechanical coupling coefficient for the device was 1.3% in the range of 3–5 V applied bias. The maximum observed quality factor was approximately 10. © *2012 American Vacuum Society*. [http://dx.doi.org/10.1116/1.4757129]

I. INTRODUCTION

Resonator devices are important components for radio frequency (RF) applications. Current technology surface acoustic wave (SAW) and bulk acoustic wave (BAW) resonators are based on piezoelectric materials such as aluminum nitride. These aluminum nitride based resonators are passive, fixed-frequency devices, which are neither tunable nor switchable. Recently, there have been demonstrations of voltage induced electrostrictive resonance in thin films of perovskite materials which are not inherently piezoelectric, such as $SrTiO_3$[1,2] and $Ba_xSr_{1-x}TiO_3$.[3–7] Voltage controlled resonator devices have been demonstrated using either free-standing film[3] or solidly mounted resonator (SMR)[2,5,7] device geometries. These studies demonstrate the potential to develop RF resonators that can be switched on/off or frequency-tuned using a low voltage control signal. The resulting components could reduce cost and increase performance for RF systems in a wide range of communications, radar, and wireless data applications.

Previous work on voltage controlled resonator devices was done using films prepared by pulsed laser deposition[3,7] or magnetron sputtering.[1,2,5] To our knowledge, there are no published reports of voltage-induced resonance for metal organic chemical vapor deposition (MOCVD) films. Investigation of acoustic resonance in MOCVD complex oxide films is significant for several scientific and technological reasons. MOCVD has the potential to produce higher quality complex oxide films than either sputtering or pulsed laser deposition, since no energetic ions are involved in the deposition process. Furthermore, MOCVD is scalable to large substrate sizes and allows conformal film deposition over device topography. MOCVD also provides a simple and quantitative means for compositional grading,[8] which can improve dielectric properties for complex oxide films. As such, we have carried out a comprehensive study to demonstrate an MOCVD process for fabrication of voltage controlled RF resonator devices.

The active layer for the SMR device configuration was chosen to be $SrTiO_3$ which is an incipient ferroelectric material. At room temperature (RT = 25 °C), single-crystal and polycrystalline (bulk) $SrTiO_3$ has the prototypical cubic perovskite structure with a P*m*3*m* symmetry. It undergoes a structural cubic-tetragonal (I4/*mcm*) phase transformation at −168 °C due to the rotations of TiO_6 octahedra about the pseudo-cube axes.[9] $SrTiO_3$ remains in a paraelectric state down to absolute zero (−273 °C) but ferroelectric phase(s) may be stabilized in $SrTiO_3$ by uniaxial stresses, external electrical fields, doping, and through in-plane misfit strains in epitaxial films.[10–14]

II. EXPERIMENT

Figure 1 shows a diagram of the solidly mounted resonator device. The substrate was (0001) sapphire (c-cut α-Al_2O_3) single crystal. The acoustic Bragg reflector consisted of four layers of SiO_2 and three layers of Ta_2O_5. The target frequency for the resonator was 5 GHz, which corresponds to a quarter wavelength thickness of 211 nm in SiO_2

[a]Electronic mail: sbrockey@structuredmaterials.com

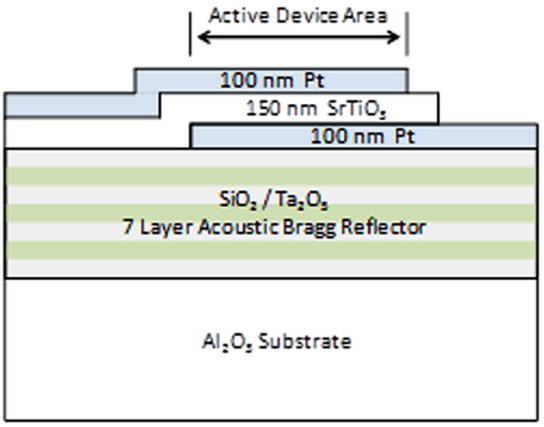

FIG. 1. (Color online) Schematic diagram of the solidly mounted resonator device fabricated with MOCVD deposited $SrTiO_3$ film.

and 163 nm in Ta_2O_5. The Bragg reflector was fabricated using metal organic solution deposition (MOSD). After depositing each SiO_2 or Ta_2O_5 layer, the film was dried at 180 °C for 2 min and baked at 280 °C for 4 min. The lower electrode layer was formed using DC magnetron sputtering. An adhesion layer of 10 nm titanium was deposited, followed by annealing at 800 °C in oxygen for 30 min. Platinum film of thickness 100 nm was then deposited by DC magnetron sputtering. The lower electrode metallization was patterned using standard photolithography and ion milling.

MOCVD of the $SrTiO_3$ films was done in a cold wall reactor, using a liquid injection, flash evaporation technique, which was previously optimized for tunable dielectric films.[8] The metalorganic precursors were $Ba(thd)_2$, $Sr(thd)_2$, and $Ti(i\text{-}OPr)_2(thd)_2$, in which "thd" and "i-OPr" represent 2,2,6,6-tetramethyl-3,5-heptanedionato and isopropoxide, respectively. The precursors were dissolved in a mixture of tetrhydrofuran plus 10% tetraethylene glycol dimethyl ether for injection into the flash evaporator. The MOCVD process pressure was 1065 Pa with a susceptor temperature of 680 °C. Additional samples of $SrTiO_3$ films were deposited using a similar process, on bare (0001) sapphire and on platinum coated silicon substrates [150 nm Pt/20 nm TiO_2/300 nm thermal SiO_2/(100) Si] for materials characterization. All MOCVD $SrTiO_3$ film samples were postannealed for 1 h at 800 °C in air. The thickness of the $SrTiO_3$ films was 150 nm as verified by Rutherford backscattering analysis of films deposited on bare (0001) sapphire.

The $SrTiO_3$ film samples deposited on sapphire and platinum coated silicon were characterized by x-ray diffraction (XRD), scanning electron microscopy (SEM), and atomic force microscopy (AFM). XRD was done using a Rigaku Geigerflex CN2013 diffraction system with Ni filtered Cu $K\alpha$ radiation. A JEOL JSM-6335 F field emission scanning electron microscope and an Asylum Research MFP-3 d atomic force microscope were used to examine the microstructure and morphology of the films as well as to calculate the root mean square (RMS) roughness.

For the $SrTiO_3$ films prepared on the solidly mounted resonator substrates for electrical characterization, a top electrode consisting of 100 nm platinum film was deposited by DC magnetron sputtering. No titanium adhesion layer was used for the top electrode. The platinum film was patterned to result in a 40 μm by 40 μm active device area. The $SrTiO_3$ film was then patterned to expose a contact to the bottom electrode.

All electrical characterization was performed at room temperature. Current–voltage (I-V) and capacitance–voltage (C-V) characteristics were measured using an HP 4110 Picoammeter and a 4275 A multifrequency LCR meter, respectively. The excitation frequency was 1.0 MHz with an amplitude of 100 mV peak to peak. Analysis of the one-port RF return loss parameter (S_{11}) was performed using an Agilent PNA vector network analyzer. The resonator device was probed with coplanar ground-signal-ground cascade microprobes. The top electrode was connected to the signal line and the bottom electrode was connected to ground. The DC bias voltage was applied by the network analyzer during the RF measurement, between the top and bottom electrodes, which corresponds to between signal and ground. The measurement setup was first calibrated from 1 to 20 GHz using matched open and shorted device structures on the same substrate. For the I-V scans, the maximum applied voltage bias was 4.4 V. For the C-V and S_{11} scans, the maximum applied voltage bias was 5.0 V.

III. RESULTS AND DISCUSSION

A. Results

Figure 2 shows XRD results for an MOCVD deposited $SrTiO_3$ film on uncoated sapphire. The results indicate the $SrTiO_3$ film to be highly (111) textured. No diffraction peaks for any other $SrTiO_3$ orientations or extraneous phases were observed. For the platinum coated silicon and platinum coated sapphire substrates used in this work, the platinum films were (111) oriented. XRD analysis of MOCVD deposited $SrTiO_3$ films on these Pt/silicon and Pt/sapphire substrates also showed the $SrTiO_3$ film to be highly (111) textured. In these cases, the $SrTiO_3$ (111) and Pt (111) peaks very nearly overlap, due to the close lattice match between $SrTiO_3$ and platinum. Similar to the films on uncoated sapphire, no diffraction peaks other than the $SrTiO_3$ (111) or

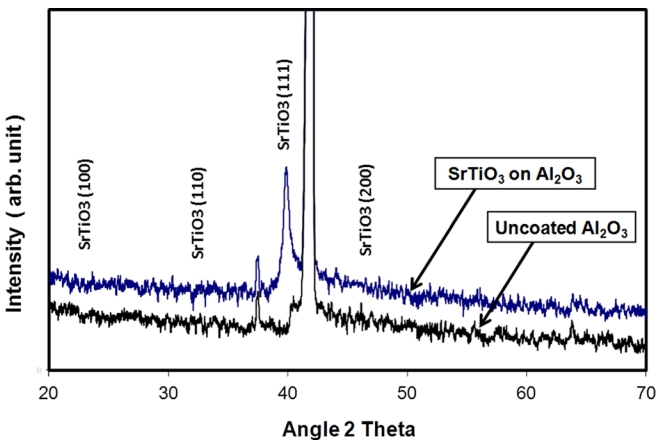

FIG. 2. (Color online) X-ray diffraction results for MOCVD deposited $SrTiO_3$ film on (0001) sapphire, compared to an uncoated sapphire substrate.

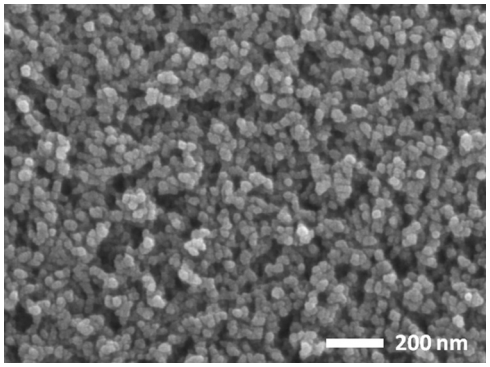

FIG. 3. Plane-view field emission SEM image of a representative $SrTiO_3$ film deposited on platinum coated silicon by MOCVD.

those attributable to the substrate were observed, indicating the $SrTiO_3$ films to be phase-pure and highly (111) textured.

Figures 3 and 4 show representative SEM and AFM results for the MOCVD $SrTiO_3$ films on platinum coated silicon. The average grain size of the $SrTiO_3$ film is 30 nm, as measured from the SEM images. The measured RMS surface roughness for the MOCVD deposited $SrTiO_3$ films on platinum coated silicon was 13.5 nm. The measured RMS surface roughness for the substrates prior to deposition of the $SrTiO_3$ film was 2.56 nm for Pt/silicon and 0.57 nm for Pt/sapphire.

Figure 5 shows I-V scan results for the $SrTiO_3$ films on the solidly mounted resonator substrate. A low leakage current of 1.6×10^{-6} A/cm^2 at 4.4 V (293 KV/cm) is observed. Figure 6 shows the dielectric constant versus applied field, as calculated from the C-V results for the $SrTiO_3$ film on the solidly mounted resonator substrate. The characteristic behavior for a paraelectric film is observed, with a maximum dielectric constant of 196 and a tunability of 43% at 330 KV/cm.

Figure 7 shows the variation of RF return loss S_{11} with frequency, as a function of DC voltage applied across the $SrTiO_3$ film. No resonance is observed with zero bias voltage. At 1.0 V bias, a well defined resonance peak is observed

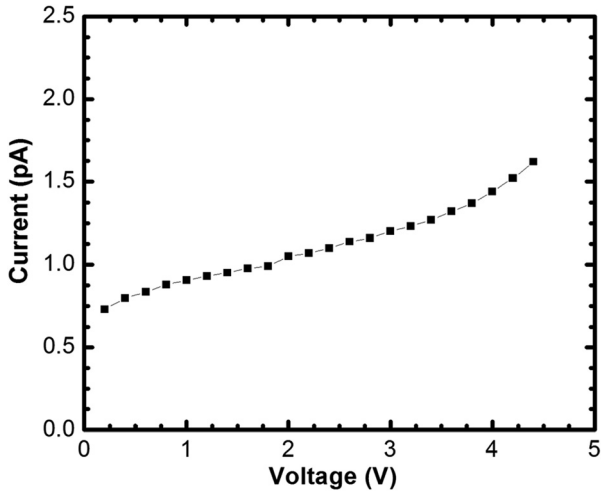

FIG. 5. DC current–voltage results for a capacitor structure with 150 nm thick $SrTiO_3$ film and platinum electrodes, demonstrating low leakage current.

at 5.606 GHz. The resonance peak increases in intensity with increasing bias voltage and shifts to lower frequency. Figure 8 shows that the decrease in resonance frequency is nearly linear with the applied bias voltage. The calculated electromechanical coupling coefficient (k^2) for the solidly mounted resonator device is 1.3%, for bias voltages in the range of 3–5 V. The maximum observed quality factor (Q) for the device was approximately 10.

B. Discussion

The electrical performance of the resonator device is expected to depend on the material properties of the paraelectric film and on device parameters such as interfacial smoothness. The MOCVD deposited $SrTiO_3$ films investigated in this study had a high degree of (111) preferred orientation, similar to $SrTiO_3$ films deposited by sputtering[15] or by chemical solution deposition[16] on (111) textured platinum coated substrates. The grain size for the MOCVD deposited

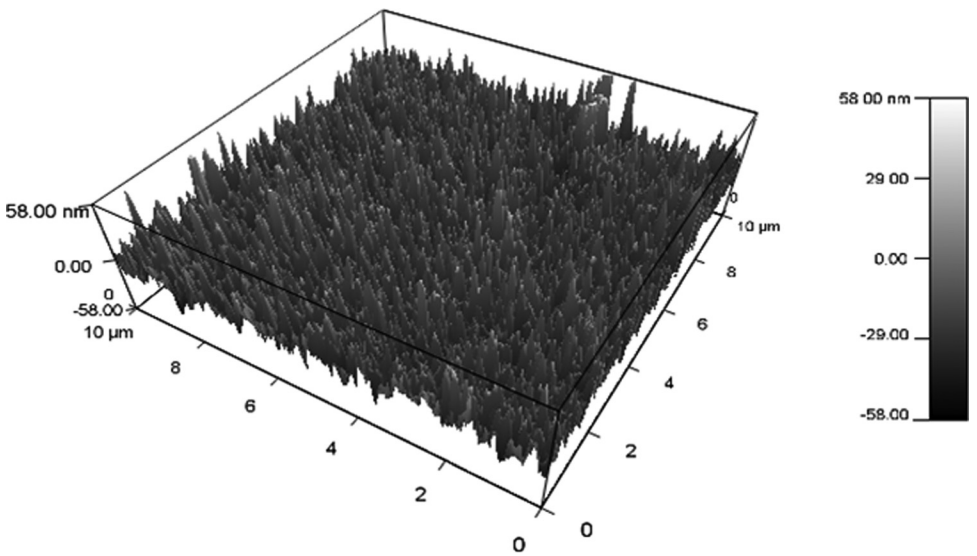

FIG. 4. AFM amplitude image of a representative $SrTiO_3$ film deposited on platinum coated silicon by MOCVD.

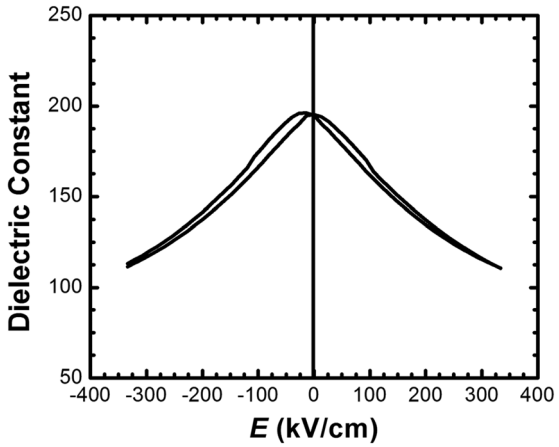

FIG. 6. Dielectric constant vs applied field, as calculated from C-V characterization of a 150 nm thick $SrTiO_3$ film and platinum electrodes.

$SrTiO_3$ films on Pt/silicon was approximately 30 nm, which is somewhat smaller than the 40–80 nm grain size reported for chemical solution deposited $SrTiO_3$ films on Pt/silicon.[17] The most pronounced difference between the MOCVD deposited $SrTiO_3$ films of this study and those prepared by other techniques was the surface roughness. The RMS surface roughness for the MOCVD deposited $SrTiO_3$ films on Pt/silicon was 13.5 nm. Other reported values for RMS roughness were 2.3 nm or less for $SrTiO_3$ films prepared by chemical solution deposition,[17] 3.1 nm or less for $SrTiO_3$ films prepared by pulsed laser deposition,[18] and 2.3 nm for $SrTiO_3$ films prepared by sputtering.[19] In this study, the large RMS roughness most likely resulted from the MOCVD process, since the measured surface roughness of the uncoated Pt/silicon substrate was 2.56 nm.

The observed dielectric properties for the MOCVD deposited $SrTiO_3$ films were comparable to those for $SrTiO_3$ films prepared by other techniques. $SrTiO_3$ films prepared by chemical solution deposition techniques have reported leakage current values ranging from 10^{-8} to 10^{-6} A/cm^2.[17,20,21] The

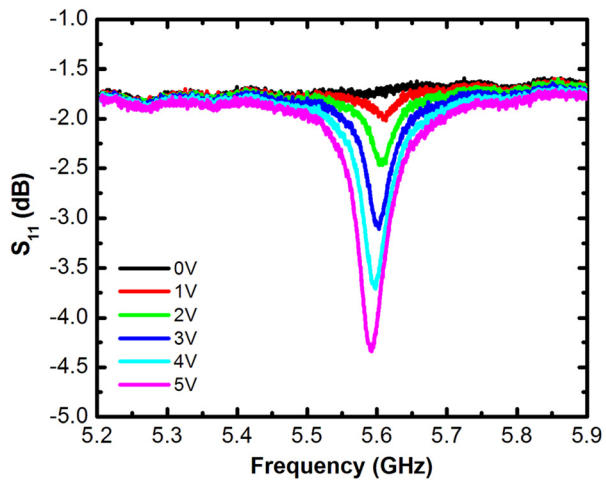

FIG. 7. (Color online) Return loss (S_{11}) for the solidly mounted resonator with 150 nm thick $SrTiO_3$ film, as a function of DC voltage across the $SrTiO_3$ film.

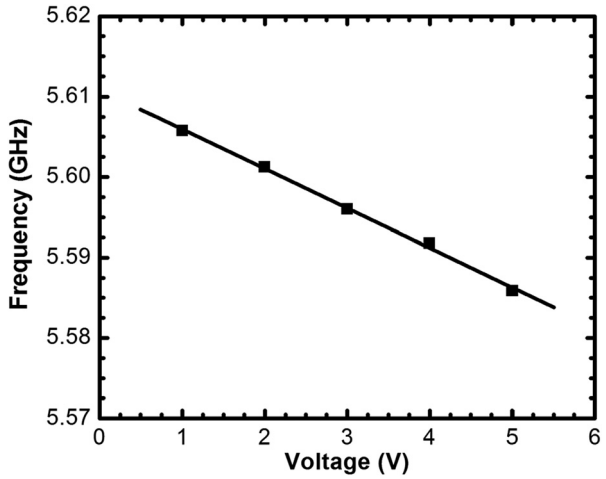

FIG. 8. Variation of resonance frequency with applied DC voltage for the $SrTiO_3$ based solidly mounted resonator.

measured dielectric constant for the MOCVD deposited $SrTiO_3$ film is also comparable to reported values for $SrTiO_3$ films prepared by chemical solution deposition techniques on platinum coated silicon substrates.[17,22] The present results are also consistent with a recent thermodynamic analysis for $SrTiO_3$ films on various substrates,[23] which predicted a dielectric constant of 265 and a tunability of 21% at 330 kV/cm, for (001) oriented $SrTiO_3$ on *c*-sapphire processed at 750 °C. These conditions are close to those for the MOCVD films of this study, since the SMR substrates were *c*-sapphire and the final annealing temperature was 800 °C. However, the MOCVD deposited $SrTiO_3$ films of the present study had a (111) preferred orientation, so some difference in results is to be expected.

The solidly mounted resonator device fabricated in this work using MOCVD deposited $SrTiO_3$ demonstrated a Q factor of about 10 and k^2 equal to 1.3% at 5 V. These results are comparable to similar SMR structures fabricated using sputtered $SrTiO_3$ films, in which k^2 was reported as 2% at 8 V.[2] Other SMR devices fabricated using sputter deposited $Ba_xSr_{1-x}TiO_3$ films yielded higher k^2 values, reported at 4% at 40 V.[5] The higher k^2 value for $Ba_xSr_{1-x}TiO_3$ as compared to $SrTiO_3$ is consistent with a recent theoretical analysis of acoustic resonance in perovskite films,[24] which showed k^2 to increase with the Ba content in $Ba_xSr_{1-x}TiO_3$ films.

Both Q and k^2 for a similar resonator device fabricated with $Ba_xSr_{1-x}TiO_3$ film were found to depend on the surface roughness of the lower electrode layer.[25] In the present study, the measured RMS surface roughness of the uncoated lower electrode layer was relatively low at 0.57 nm for Pt/sapphire and 2.56 nm for Pt/silicon. However, the surface roughness of the deposited and annealed $SrTiO_3$ film was relatively high at 13.5 nm. This would result in a rough interface between the $SrTiO_3$ film and the upper electrode, which could negatively affect the device performance in this work. Other studies of $SrTiO_3$ film deposition found the surface roughness to depend strongly on processing conditions.[17,18] Therefore, it is reasonable to assume that further optimization of the MOCVD process could result in lower surface

roughness for the $SrTiO_3$ films and higher values of Q and k^2 for the solidly mounted resonator device.

IV. SUMMARY AND CONCLUSIONS

Voltage induced acoustic resonance is demonstrated for the first time for an MOCVD deposited film. The MOCVD deposited $SrTiO_3$ films showed bulk-like dielectric properties, similar to high quality $SrTiO_3$ films prepared by solution deposition techniques. A solidly mounted resonator device fabricated using MOCVD deposited $SrTiO_3$ was shown to turn on at an applied DC bias of 1.0 V. The acoustic resonance peak increased in intensity and shifted to lower frequency as the applied voltage increased over the range of 1.0–5.0 V. The calculated k^2 and Q values for the device were comparable to similar resonators fabricated using sputter deposited $SrTiO_3$ films. Further improvements in resonator performance should be possible by optimizing device parameters such as surface roughness of the $SrTiO_3$ film. The MOCVD film deposition technique is shown to be a viable approach for fabricating voltage controlled resonator devices using complex oxide films.

ACKNOWLEDGMENTS

This work was funded by the Army Research Office under Contract Number W911NF-11-C-0219. S.P.A. and J.Z. would like to thank Dr. Lichun Zhang and Dr. Roger Ristau (UConn—IMS) for their help with sample preparations for the SEM and AFM measurements.

[1]K. Morito, Y. Iwazaki, T. Suzuki, and M. Fujimoto, J. Appl. Phys. **94**, 5199 (2003).
[2]G. N. Saddik, D. S. Boesch, S. Stemmer, and R. A. York, Appl. Phys. Lett. **91**, 043501 (2007).
[3]X. Zhu, J. D. Phillips, and A. Mortazawi, *IEEE/MTT-S International Microwave Symposium* (IEEE, Piscataway, NJ, 2007), p. 671.
[4]S. Tappe, U. Böttger, and R. Waser, Appl. Phys. Lett. **85**, 624 (2004).
[5]G. N. Saddik and R. A. York, *IEEE/MTT-S International Microwave Symposium* (IEEE, Piscataway, NJ, 2011), p. 1.
[6]V. M. Mukhortov, S. V. Biryukov, Y. I. Golovko, G. Y. Karapet'yan, S. I. Masychev, and V. M. Mukhortov, Tech. Phys. Lett. **37**, 207 (2011).
[7]J. Berge, A. Vorobiev, W. Steichen, and S. Gevorgian, IEEE Microw. Wirel. Compon. Lett. **17**, 655 (2007).
[8]N. M. Sbrockey, M. W. Cole, T. S. Kalkur, M. Luong, J. E. Spanier, and G. S. Tompa, Integr. Ferroelectr. **126**, 21 (2011).
[9]M. Fujimoto, *The Physics of Structural Phase Transitions* (Springer, New York, 1997).
[10]H. Uwe and T. Sakudo, Phys. Rev. B **13**, 271 (1976).
[11]J. G. Bednorz and K. A. Muller, Phys. Rev. Lett. **52**, 2289 (1984).
[12]J. Hemberger, M. Nicklas, R. Viana, P. Lunkenheimer, A. Loidl, and R. Bohmer, J. Phys.: Condens. Matter **8**, 4673 (1996).
[13]N. A. Pertsev, A. K. Tagantsev, and N. Setter, Phys. Rev. B **61**, R825 (2000).
[14]J. H. Haeni *et al.*, Nature **430**, 758 (2004).
[15]D. O. Klenov, T. R. Taylor, and S. Stemmer, J. Mater. Res. **19**, 1477 (2004).
[16]C. L. Jia, K. Urban, S. Hoffmann, and R. Waser, J. Mater. Res. **13**, 2206 (1998).
[17]C. V. Weiss, J. Zhang, M. Spies, L. S. Abdallah, S. Zollner, M. W. Cole, and S. P. Alpay, J. Appl. Phys. **111**, 054108 (2012).
[18]R. Castro-Rodriguez, A. I. Oliva, M. Aguilar, P. Bartolo-Perez, E. Vasco, F. Leccabue, and J. L. Peñal, Appl. Surf. Sci. **125**, 58 (1998).
[19]M. V. Raymond, H. N. Al-Shareef, D. B. Dimos, N. Missert, C. Mueller, and D. Galt, Integr. Ferroelectr. **17**, 247 (1997).
[20]P. C. Joshi and S. B. Krupanidhi, Appl. Phys. Lett. **61**, 1525 (1992).
[21]M. N. Kamalasanan, N. D. Kumar, and S. Chandra, J. Appl. Phys. **74**, 679 (1993).
[22]F. M. Pontes, E. J. H. Lee, E. R. Leite, and E. Longo, J. Mater. Sci. **35**, 4783 (2000).
[23]J. Zhang, C. V. Weiss, and S. P. Alpay, Appl. Phys. Lett. **99**, 042902 (2011).
[24]A. Noeth, T. Yamada, A. K. Tagantsev, and N. Setter, J. Appl. Phys. **104**, 094102 (2008).
[25]G. N. Saddik, J. Son, S. Stemmer, and R. A. York, J. Appl. Phys. **109**, 091606 (2011).